CO Oxidation Kinetics over Au/TiO_2 and Au/Al_2O_3 Catalysts: Evidence for a Common Water-Assisted Mechanism

Johnny Saavedra,[a] Christopher J. Pursell,[b] and Bert D. Chandler[*,b]

[a]Current address: Institute for Integrated Catalysis, Pacific Northwest National Laboratory, Richland, WA 99352 (USA).

[b]Department of Chemistry, Trinity University, San Antonio, TX 78212-7200 (USA)

[*]To whom correspondence should be addressed:
Bert.chandler@trinity.edu (210) 999-7557 phone; (210) 999-7569 fax

Supporting Information

Table of Contents

1. Materials and Methods

1.1 Materials

The catalysts used in this study were commercial AUROlite™ samples purchased from STREM Chemicals (nominal 1% Au/TiO_2 and Au/Al_2O_3). These catalysts were pretreated by the manufacturer to ensure that particles were of appropriate size (2.9 ± 0.9 nm for Au/TiO_2, and 2.2 ± 0.7 nm for Au/Al_2O_3) to be active for CO oxidation. The catalyst was crushed and stored in a dark refrigerator. Powdered Silicon Carbide (400 mesh) was purchased from Aldrich.

Gases (N_2, H_2, O_2, and 5% CO/He) were 5.0 grade supplied by Praxair and used with no additional purification. Deuterium oxide (99.9%) was purchased from Cambridge Isotope Laboratories. Water was purified to a resistivity of 18.6 Ω with a Barnstead Nanopure system.

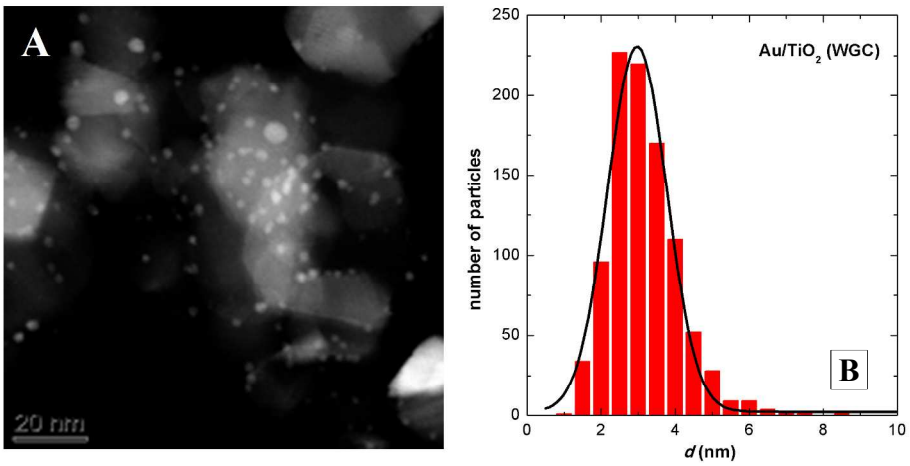

Figure S1. TEM data for Au/TiO_2. TEM micrograph (A) and Particle size distribution (B); mean calculated particle size is 2.9 ± 0.9 nm.

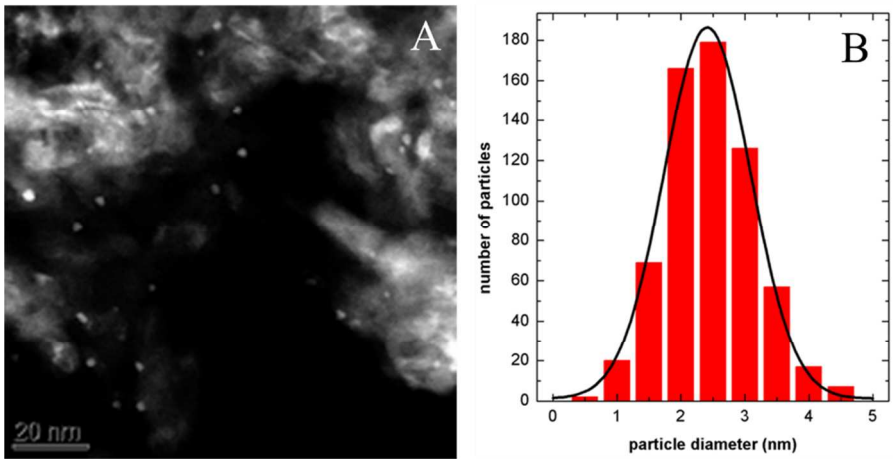

Figure S2. TEM data for Au/Al_2O_3. TEM micrograph (A) and Particle size distribution (B); mean calculated particle size is 2.2 ± 0.7 nm.

1.2 Catalyst pretreatments

Each experiment was performed with a fresh sample of catalyst. The catalyst was active with no further treatment; however, several pretreatments using N_2 were applied to the catalyst with three primary goals: 1) equilibrate the water adsorbed on the catalyst surface with a known, controlled H_2O vapor pressure, 2) expose the catalyst to a feed containing D_2O vapor in order to exchange the original OH/H_2O_{ads} species on the catalyst surface (to form OD/D_2O_{ads}), and 3) remove surface water to dry the catalyst. Table S1 summarizes the pretreatments applied to the catalyst immediately prior to reactivity and IR studies.

Table S1. Catalyst Pretreatments.

Procedure	N_2 Flow (mL/min)	Conditions
a. H_2O saturation	100	30 min (N_2+700 Pa H_2O) + 30 min (N_2) at 20 °C
b. Isotope Interchange	100	30 min (N_2+700 Pa D_2O) + 30 min (N_2) at 20 °C
g. Complete Drying (loosely bound water)	100	1 hr (N_2) at 120°C

1.3 Catalysis experiments

CO Oxidation Catalysis. The CO oxidation reactor consisted of a home-built laboratory scale single pass plug-flow micro-reactor. The reaction zone consisted of finely ground fresh catalyst (4 mg Au/TiO_2 or 12 mg Au/Al_2O_3) diluted in 750 mg of silicon carbide. Gas flows were controlled with 4 electronic low pressure mass flow controllers (Porter Instruments). The composition of the feed and reactor effluent (CO and CO_2) was determined using a Siemens Ultramat 23 IR gas analyzer.

After loading into a glass U-tube, the diluted catalyst was stabilized for 4h with variable contents of moisture in the gas (0.1 to 700 Pa). CO oxidation activity was measured in a 60 min experiment immediately following the pretreatment. The feed (1% CO, 20% O_2, balance N_2, 180 mL/min; WHSV = 2.2 x 10^3 L/h/g_{cat}) was held constant and the reaction temperature was maintained at 20 ºC using a water bath.

Gases and their analytical mixtures may contain water in ppm levels. Moisture in the gaseous feeds used in these experiments was controlled using a coil submerged into a dry ice trap (-78.5 °C). In this way, water pressure can be decreased to an approximate value of 0.1 Pa, which corresponds to the equilibrium vapor pressure at the temperature of the dry ice. Moisture in the gas was controlled by subsequently passing the gas through a water column submerged in a dry ice / isopropanol bath set at a constant, but adjustable temperature (-78.5 to 20 °C).

a. **H_2O reaction order.** The H_2O reaction order measurements were performed under CO oxidation catalysis conditions shown above. Prior to CO oxidation measurements, water adsorbed on the catalyst was equilibrated with N_2 (100 mL/min) containing variable amounts of water vapor for 4 hours. The water vapor content in the N_2 (1, 5, 20, 50, 125 Pa) was changed using a saturator set at different temperatures.

b. O_2 kinetic dependence. The O_2 dependence measurements used in the Michaelis-Menten kinetic analyses were performed using five different O_2 contents (10, 15, 18, 20, 24 $\%_{vol}$). Prior to each kinetics experiment, the catalyst was equilibrated with H_2O/N_2 for 4 hours with variable amounts of moisture in the gas (1, 5, 20, 50, 125 Pa).

c. CO reaction order. CO kinetic dependence was performed using five CO contents (0.56, 0.8, 1.0, 1.2, and 1.4$\%_{vol}$) at 0 and 60 Pa of water vapor. O_2 content was held constant at 20%.

1.4 Infrared spectroscopy

A previously described home built flow IR cell was used for the *in situ* FTIR experiments.[1-5] The cell consisted of a stainless steel chamber wrapped by a heating mantle (up to 400ºC) with two IR transparent KBr windows. Gases were mixed in an external stainless steel manifold using low pressure rotameters. The gas cell was fed with 100 mL/min of gas mixtures and heated at a constant rate of 5º C/min.

The catalyst (~25 mg) was finely ground in an agate mortar, pressed into a 13 mm circular pellet using a stainless steel die and a manual hydraulic press (5 metric tons of pressure for 2 min). The pellet was mounted into the cell and placed in the sample compartment of a Nicolet FTIR spectrometer where a thermocouple adjacent to the pellet monitored the temperature.

Prior to any treatment, a background spectrum of the catalyst pellet in the sample cell was collected. The catalyst pretreatment was carried out *in situ* using 100 mL/min of the gas mixture at different temperatures (150, 250 and 350 ºC; WHSV= 2.00 x 10^2 $L \cdot h^{-1} \cdot g_{cat}^{-1}$). After treatment, the sample was purged for 1 hr and cooled to room temperature under N_2 flow. Spectra were collected at 20 ºC and the temperature was kept constant using a coil with recirculating water.

Immediately after treatment, the sample was cooled and a reference spectrum was collected once the temperature was equilibrated at 20 ºC. To measure water adsorption isotherms, the moisture in the gas was controlled by passing the feed through a water column submerged in a dry ice / isopropanol bath set at a constant, but adjustable temperature (-78.5 to 20 °C).

The catalyst pellet was then used for the in situ CO oxidation reaction. The CO oxidation reaction consisted of 4 steps: (a) 10 min flowing with a 1% CO mixture, (b) 10 min with our standard CO oxidation mixture (1% CO, 20% O_2), (c) 10 min flowing with a 1% CO, and (d) 10 min purging with N_2. Spectra were collected every 2.5 min.

1.5 Thermogravimetric analysis (TGA) experiments

The amount of water adsorbed on the catalyst was determined using a TGA-50 Shimadzu Thermogravimetric Analyzer. Finely ground catalyst (4 mg) was placed in the aluminum sample holder. Using a 5 °C/min ramp, the sample was heated from room temperature to 120 °C, held at 120 °C for 1 hr, and heated to 250 °C. The sample weight was recorded continuously during the heating treatment.

2. H/D Isotope exchange and kinetic isotope effect (KIE)

H/D exchange was accomplished by passing an N_2 feed (100 mL/min) through a water saturator thermostatted at 5 °C to produce a 700 Pa D_2O/N_2 feed. This feed was then contacted with a catalyst pellet (30 mg) and placed in an *in-situ* IR spectroscopy cell. The exchange process was followed with IR spectroscopy to monitor the degree of exchange (Fig. S3).

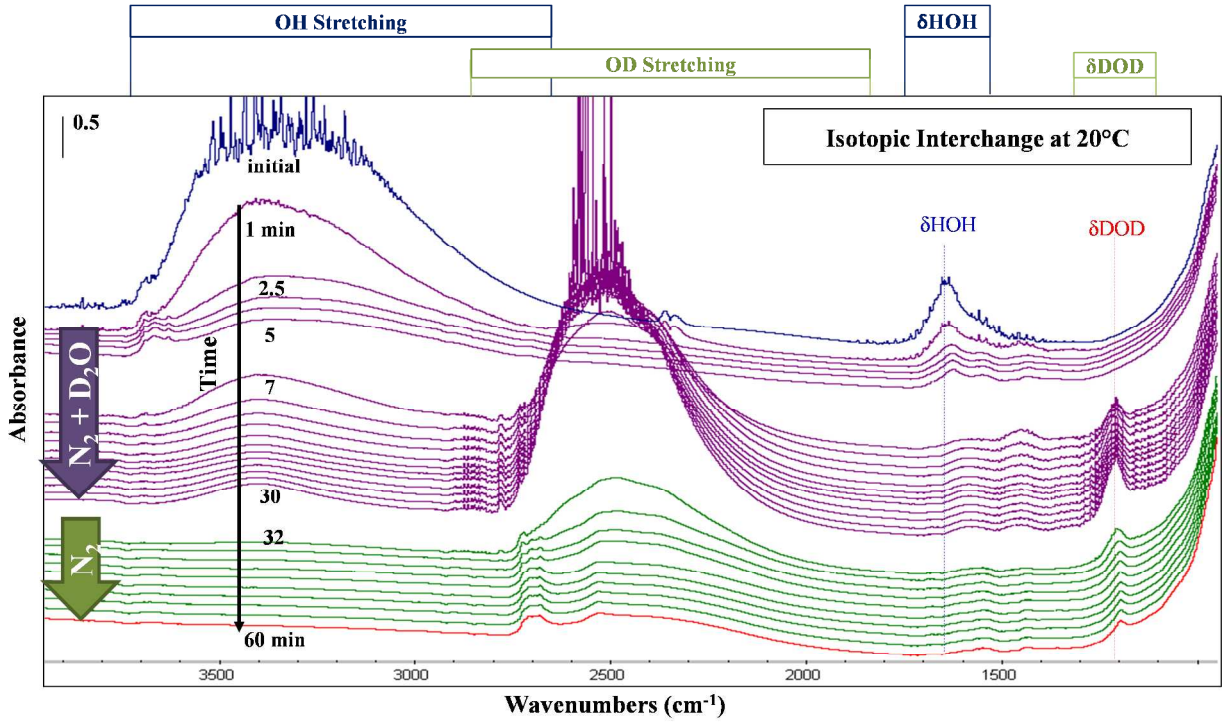

Figure S3. FTIR spectra during isotopic exchange of Au/TiO_2 wafer at 20°C under flowing D_2O / N_2 (100 mL/min, 700 Pa of D_2O).

The top (blue) spectrum in Fig. S3 shows a fresh Au/TiO_2 catalyst. The δ_{HOH} bending vibrations centered at 1623 cm^{-1} are exclusively due to adsorbed water. The broad high frequency band (3800- 2600 cm^{-1}) is due to hydrogen-bonded OH stretching arising from interactions between adsorbed water molecules and possibly surface hydroxyl groups. The small shoulder on this band (~3670 cm^{-1}) is due to non hydrogen-bonded surface Ti–OH groups. Small peaks in the 1400-1600 cm^{-1} region are attributed to small amounts of surface carbonates, which are common for these materials.[5]

Upon contact with the 700 Pa D_2O/ N_2 feed, the bands associated with adsorbed H_2O and surface Ti-OH attached to the support quickly disappear and are replaced by the corresponding OD stretching (2800-1800 cm^{-1}), δ_{DOD} bending (1200 cm^{-1}), and δHOD bending (1430 cm^{-1}) bands (purple spectra).[6] This appears to be an extremely facile process, as the only observed delay is the time it takes for the wet gas to travel through the gas lines. This exchange is largely complete 10 minutes after the initial contact with D_2O. After 30 minutes of interchange, all the adsorbed H_2O was removed from the sample (monitored by disappearance of δ_{HOH} band at 1623

cm^{-1}). A small amount of HOD likely accounts for the remaining broad O-H stretching (symmetrical band centered at 3400 cm^{-1}) observed as δ_{HOD} bending is also observed.[6] The D_2O was removed from the gas feed and the sample was flushed for additional 30 minutes with N_2 (green spectra in Fig. S3) until no further changes occurred to the spectrum. After this N_2 flush, no δ_{HOH} modes are observed and only a trace of O-H stretching modes are observed, indicating that, at least to the detection limit of infrared spectroscopy, all of the adsorbed H_2O had been removed.

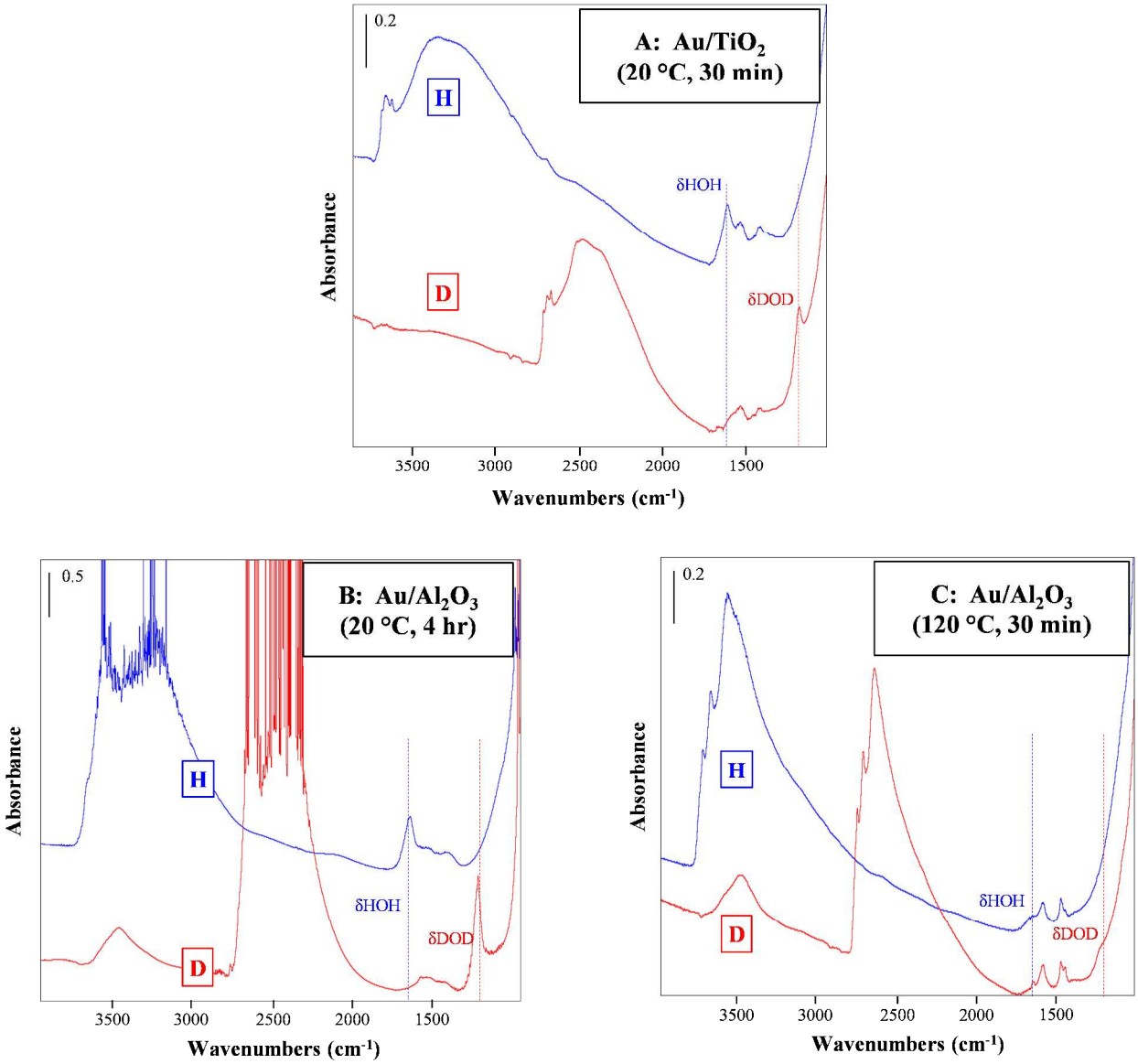

Figure S4. Changes in FTIR spectra showing D_2O treatment of an (A) Au/TiO_2 (30 mg) wafer at 20 °C, (B) an Au/Al_2O_3 wafer (~20 mg) at 20 °C, and (C) an Au/Al_2O_3 wafer (~20 mg) at 120 °C The top (blue) spectrum was collected after H_2O saturation; the bottom (red) spectrum was collected after D_2O exchange.

The net exchange process is summarized in Fig. S4, which shows two spectra for each catalyst. Panel A shows a spectrum of the sample after it had been saturated with 700 Pa of H_2O for 30 min and then flushed with N_2 for 30 min to remove the vapor phase water (top, blue), and a spectrum of the same pellet after exchange with 700 Pa of D_2O for 30 min followed by flushing with N_2 for 30 min to remove the vapor phase D_2O (bottom, red). The exchange on Au/Al_2O_3 was slower, likely due to the higher surface area and more complicated pore structure. Complete H/D exchange required flowing D_2O for 4 hours at 20 °C (panel B). The exchange could also be completed in 30 minutes by increasing the temperature to 120 °C (panel C).

The red spectrum in each panel shows that these conditions allow for essentially complete exchange of all –OH(D) groups on the surface (at least to the detection limit of IR spectroscopy) as there are few observable OH stretches remaining (likely due to HOD). Additionally, the area under the –OH spectrum and the area under the –OD spectrum in panels A and C are within 10% of each other, indicating complete H/D exchange. The saturation of the IR signal in panel B did not allow this comparison to be made for the room temperature treatment of the Au/Al_2O_3 catalyst.

3. Additional Kinetics and Spectroscopy Data

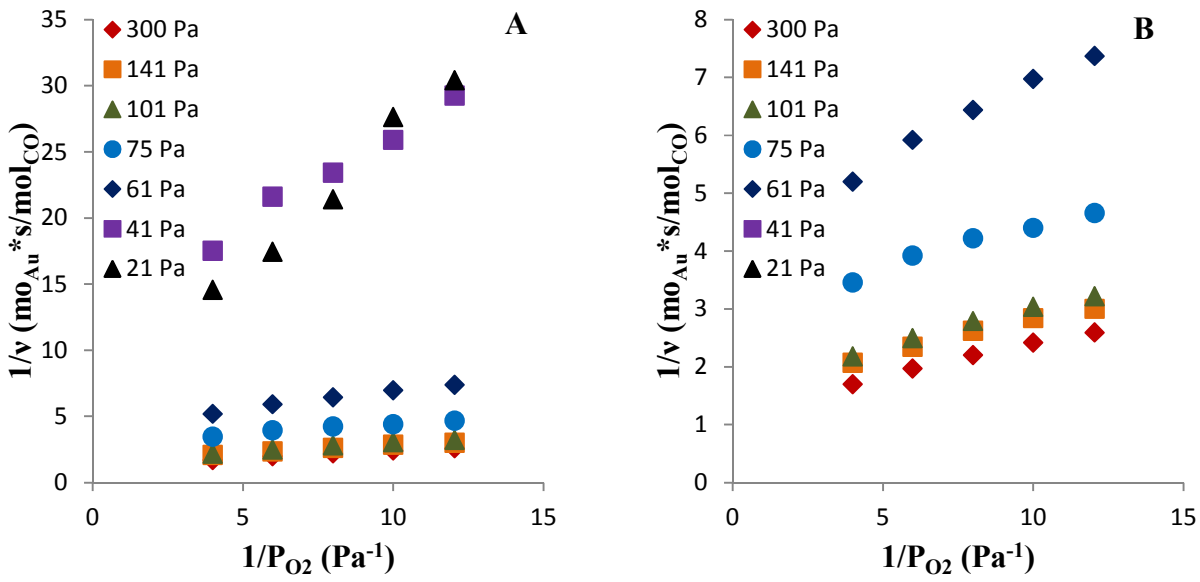

Figure S5. (A) Double reciprocal plots for the O_2 dependence data from Au/Al_2O_3 showing all the water pressures (legend) studied. (B) Double reciprocal plots presented in the main text.

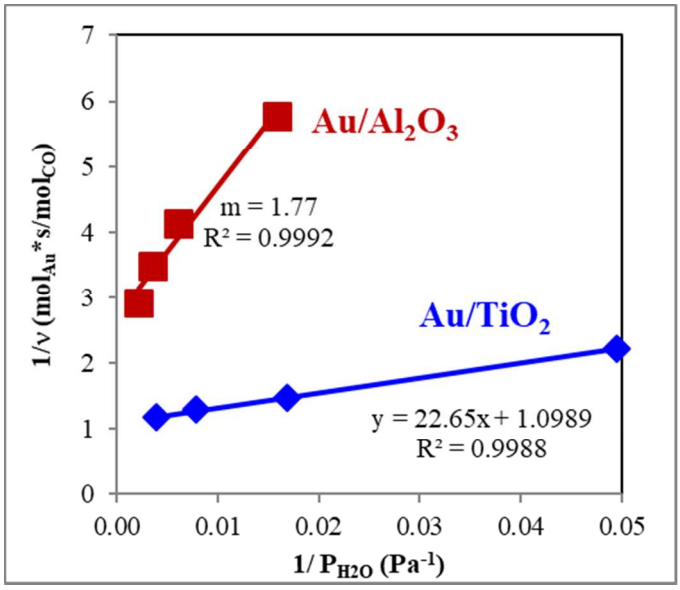

Figure S6. Double reciprocal plots for the H_2O dependence data from the Au/Al_2O_3 and Au/TiO_2 catalysts.

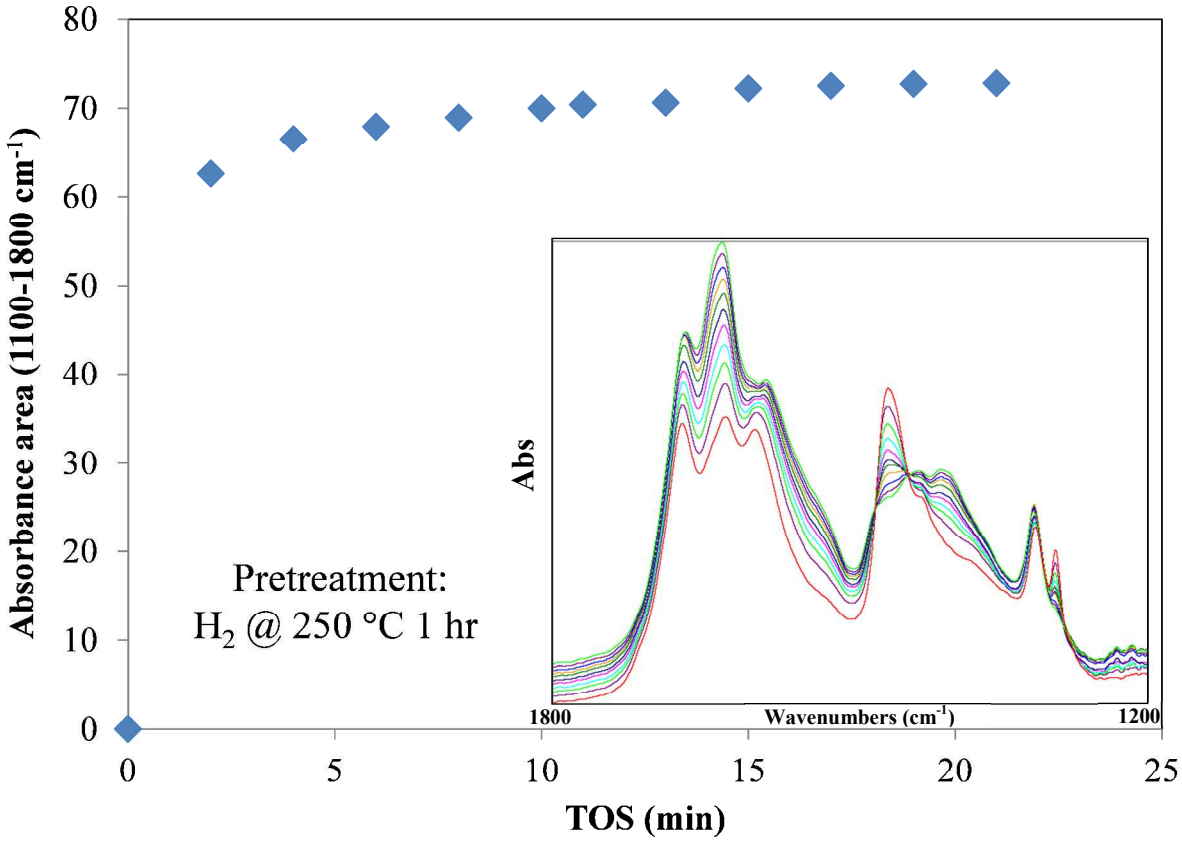

Figure S7. IR spectra showing growth of carbonates peaks during CO oxidation catalysis over Au/TiO_2. The catalyst was pretreated with H_2 at 250 °C for 1 hour; this pretreatment has previously been shown to generate large amounts of carbonates and eliminate most of the catalytic activity.

4. Rate Law Derivation

Proposed mechanism for catalytic CO oxidation over supported gold nanoparticles with support-adsorbed water as a co-catalyst.[7]

Mechanistic steps:

1. $2\left(Au' + CO \overset{K_1}{\leftrightarrow} Au' - CO\right)$

2. $Au^* + Supp_{MSI} + H_2O \overset{K_2}{\leftrightarrow} Au^*(H_2O)_{MSI}$

3. $Au^*(H_2O)_{MSI} + O_2 \overset{K_3}{\leftrightarrow} Au^* - OOH + (OH^-)_{MSI}$

4. $Au^* - OOH + Au' - CO \overset{K_4}{\leftrightarrow} Au' - COOH + Au^* - O$

5. $Au' - COOH + (H_2O)_{MSI} \overset{k_5}{\rightarrow} Au' + CO_2 + (H_3O^+)_{MSI}$ RDS

6. $Au^* - O + Au' - CO \overset{k_6}{\rightarrow} Au + Au' + CO_2$ $very\ fast\ step$

7. $(OH^-)_{MSI} + (H_3O^+)_{MSI} \overset{K_w}{\rightarrow} 2\,(H_2O)_{MSI}$ $very\ fast\ step$

overall reaction: $2\,CO + O_2 \rightarrow 2\,CO_2$

This mechanism involves four fast, reversible, pre-equilibrium steps:

Step 1. Adsorption of carbon monoxide on the gold nanoparticles at low-coordinate sites near the metal-support interface (MSI).

Step 2. The interaction of water with the support at the MSI. This positions the water co-catalyst close to the Au nanoparticle and gives rise to the arrangement of the Au and water that allows for oxygen activation. This equilibrium is essentially the same as water adsorption on the remainder of the support; thus, he fraction of Au* sites available for O_2 adsorption should be roughly equivalent to the water coverage on the bulk of the support.

Step 3. Oxygen activation at the MSI. In this process a proton is transferred from the interface water to the oxygen forming the activated oxygen species $Au^* - OOH$. The amount of OH^- formed in this step on the support at the interface with the gold nanoparticles is assumed to be approximately constant and is incorporated into the K_3 equilibrium constant as K_3' (see below).

Step 4. Reaction between the two primary adsorbed reactive species leading to the formation of the $Au' - COOH$ species. Because step 6 is very fast, the amount of $Au^* - O$ is considered very small and constant, and is therefore incorporated into the K_4 equilibrium constant as K_4' (see below).

Step 5. Rate determining decomposition of the $Au' - COOH$ reactive species and the production of the first equivalent of CO_2. This step involves a proton transfer from COOH to water at the metal-support interface and is consistent with our recent DFT calculations and experimental KIE results.[7]

Step 6. The $Au^* - O$ species formed in step 4 reacts quickly with adsorbed CO leading to formation of the second equivalent of CO_2. This step is required to close the catalytic cycle and its low barrier is supported by a large number of DFT calculations.[8-13]

Step 7. The $(OH^-)_{MSI}$ and $(H_3O^+)_{MSI}$ species formed in steps 3 and 5, respectively, undergo a rapid proton transfer to regenerate two equivalents of water. This step is required to close the catalytic cycle and is assumed to be fast, as water autodissociation is generally considered to be.

Based upon this mechanism, we define the following pre-equilibrium constants:

$$K_1 = \frac{[Au' - CO]}{[Au']P_{CO}}$$

$$K_2 = \frac{[Au^*(H_2O)_{MSI}]}{[Au^*][Supp_{MSI}]P_{H_2O}} = K_{wH2O} = \frac{[(H_2O)_{MSI}]}{[Supp_{MSI}]P_{H_2O}}$$

$$K_3 = \frac{[Au^* - OOH][(OH^-)_{MSI}]}{[Au^*(H_2O)_{MSI}]P_{O_2}}$$

$$K_3' = \frac{K_3}{[(OH^-)_{MSI}]} = \frac{[Au^* - OOH]}{[Au^*(H_2O)_{MSI}]P_{O_2}} \qquad since\ [(OH^-)_{MSI}] \approx constant$$

$$K_4 = \frac{[Au' - COOH][Au^* - O]}{[Au^* - OOH][Au' - CO]}$$

$$K_4' = \frac{K_4}{[Au^* - O]} = \frac{[Au' - COOH]}{[Au^* - OOH][Au' - CO]} \qquad since\ [Au^* - O] \approx constant$$

The experimental reaction rate is given by step 5, the rate determining step, as

$$Rate = k_5\theta_{H_2O}[Au' - COOH]$$

Where θ_{H_2O} is the coverage of water on the support. This assumes that the fractional occupancy of the support MSI sites is the same as the water coverage over the support.

$$from\ K_4' : \quad [Au' - COOH] = K_4'[Au^* - OOH][Au' - CO]$$

Therefore,

$$I. \quad Rate = k_5 K_4' \theta_{H_2O} [Au^* - OOH] [Au' - CO]$$

This important expression shows that the experimental rate depends on the surface concentration of the "activated" oxygen species, on the amount of adsorbed water on the support at the metal-support interface (MSI), and on the surface concentration of CO adsorbed near the MSI.

Using a site balance expression for the total number of gold sites available to bind and activate oxygen:

$$[Au_T^*] = [Au^*] + [Au^*(H_2O)_{MSI}] + [Au^* - OOH] + [Au^* - O]$$

We assume that the fraction of Au* sites with access to water is proportional to the water coverage on the support, in the same fashion that we assumed that the support MSI site coverage was equivalent to the bulk water coverage on the support. This expression can be simplified to:

$$\theta_{H_2O}[Au_T^*] = [Au^*(H_2O)_{MSI}] + [Au^* - OOH] + [Au^* - O]$$

Using the expression for K_3' for the $[Au^*(H_2O)_{MSI}]$ species and assuming $[Au^* - O]$ is constant and small relative to the other species (*ca.* because step 6 is very fast), $[Au_T^*]$ becomes,

$$\theta_{H_2O}[Au_T^*] = \frac{[Au^* - OOH]}{K_3' P_{O_2}} + [Au^* - OOH]$$

Solving for $[Au^* - OOH]$ yields the Langmuir-like expression for coverage of this species,

$$II. \quad [Au^* - OOH] = \frac{\theta_{H_2O}[Au_T^*] K_3' P_{O_2}}{1 + K_3' P_{O_2}}$$

Now considering the site balance for the total number of gold sites for CO adsorption,

$$[Au_T'] = [Au'] + [Au' - CO]$$

Using the expression for K_1 for the $[Au']$ species gives,

$$[Au_T'] = \frac{[Au' - CO]}{K_1 P_{CO}} + [Au' - CO]$$

Solving for $[Au' - CO]$ yields the Langmuir-like expression for coverage of this species,

$$III. \quad [Au' - CO] = \frac{[Au_T'] K_1 P_{CO}}{1 + K_1 P_{CO}}$$

Substituting expressions II and III into expression I produces the Langmuir-Hinshelwood-like expression for the rate of reaction,

$$IV. \quad Rate = k_5 K_4' \theta_{H_2O} \left\{ \frac{K_3' P_{O_2}}{1 + K_3' P_{O_2}} \theta_{H_2O} [Au_T^*] \right\} \left\{ \frac{K_1 P_{CO}}{1 + K_1 P_{CO}} [Au_T'] \right\}$$

This expression is essentially the Langmuir-Hinshelwood expression where the rate depends on adsorbed water, activated oxygen coverage, and adsorbed carbon monoxide coverage. Under our experimental conditions $K_1 P_{CO} \gg 1$, therefore the last term reduces to $[Au_T']$ (*cf.* this term represents the total number of CO binding sites in close proximity to the O_2 binding sites). The overall rate then becomes,

$$V. \quad Rate = k_5 K_4' \theta_{H_2O} [Au_T'] \left\{ \frac{K_3' P_{O_2}}{1 + K_3' P_{O_2}} [Au_T^*] \right\}$$

and inverting this rate expression in order to create a double-inverse expression,

$$VI. \quad \frac{1}{Rate} = \frac{1}{k_5 K_4' \theta_{H_2O} [Au_T'][Au_T^*]} \left(\frac{1}{K_3' P_{O_2}} \right) + \frac{1}{k_5 K_4' \theta_{H_2O} [Au_T'][Au_T^*]}$$

At constant water pressure, ν_{max} and K_R can be defined as as,

$$\nu_{max} = k_5 K_4' \theta_{H_2O} [Au_T'][Au_T^*] \quad \text{and} \quad K_R = 1/K_3'$$

The expression simplifies to:

$$VII. \quad \frac{1}{Rate} = \frac{K_R}{\nu_{max}} \left(\frac{1}{P_{O_2}} \right) + \frac{1}{\nu_{max}}$$

The rate law can be further expanded to incorporate water adsorption at the MSI by considering water adsorption on the support at the MSI:

$$7. \quad H_2O + Supp_{MSI} \overset{K_{H2O}}{\longleftrightarrow} (H_2O)_{MSI}$$

Using a site balance expression for the total number of water binding sites on the support at the MSI:

$$[Supp_{MSI}]_T = [Supp_{MSI}] + [(H_2O)_{MSI}]$$

and the equilibrium constant associated with water adsorption on the support at the MSI:

$$K_{H_2O} = \frac{[(H_2O)_{MSI}]}{P_{H_2O}[Supp_{MSI}]}$$

the concentration of water at the MSI can be expressed as:

$$[(H_2O)_{MSI}] = \frac{K_{wH_2O}P_{H_2O}}{1 + K_{wH_2O}P_{H_2O}}[Supp_{MSI}]_T$$

Or

$$\frac{[(H_2O)_{MSI}]}{[Supp_{MSI}]_T} = \frac{K_{wH_2O}P_{H_2O}}{1 + K_{wH_2O}P_{H_2O}} = \theta_{H_2O}$$

The rate law can then be expressed as:

$$VIII.\ Rate = k_5 K_4' \left\{\frac{K_{wH_2O}P_{H_2O}}{1 + K_{wH_2O}P_{H_2O}}\right\}\left\{\frac{K_3' P_{O_2}}{1 + K_3' P_{O_2}}[Au_T^*]\right\}\left\{\frac{K_1 P_{CO}}{1 + K_1 P_{CO}}[Au_T']\right\}$$

Under constant O_2 and CO pressures, the O_2 and CO Langmuir-Hinschelwood terms become constant, allowing the rate law to be simplified to:

$$Rate = k_5 K_4' [Au_T^*][Au_T']\left\{\frac{K_{wH_2O}P_{H_2O}}{1 + K_{wH_2O}P_{H_2O}}\right\}$$

A double reciprocal plot of this equation yields

$$\frac{1}{Rate} = \frac{1}{k_5 K_4' [Au_T'][Au_T^*]K_{wH_2O}}\left(\frac{1}{P_{H_2O}}\right) + \frac{1}{k_5 K_4' [Au_T'][Au_T^*]}$$

A value for K_{wH2O} can then be determined at each O_2 pressure from the slope and intercept of each of this linear form of the equation.

References

1. Korkosz, R. J.; Gilbertson, J. D.; Prasifka, K. S.; Chandler, B. D., Dendrimer Templates for Supported Au Catalysts. *Catalysis Today* **2007,** *122*, 370-377.

2. Singh, A.; Chandler, B. D., Mild Thermolysis Conditions for the Activation of Dendrimer Encapsulated Pt Nanoparticles. *Langmuir* **2005,** *21*, 10776-10782.

3. Lang, H.; Maldonado, S.; Stevenson, K. J.; Chandler, B. D., Synthesis and Characterization of Dendrimer Templated Supported Bimetallic Pt-Au Nanoparticles. *Journal of the American Chemical Society* **2004,** *126*, 12949-12956.

4. Lang, H.; May, R. A.; Iversen, B. L.; Chandler, B. D., Dendrimer Encapsulated Nanoparticle Precursors to Supported Platinum Catalysts. *Journal of the American Chemical Society* **2003,** *125*, 14832-14836.

5. Saavedra, J.; Powell, C.; Panthi, B.; Pursell, C. J.; Chandler, B. D., CO oxidation over Au/TiO2 catalyst: Pretreatment effects, catalyst deactivation, and carbonates production. *J. Catal.* **2013,** *307*, 37-47.

6. Auer, B.; Kumar, R.; Schmidt, J. R.; Skinner, J. L., Hydrogen bonding and Raman, IR, and 2D-IR spectroscopy of dilute HOD in liquid D2O. *PNAS* **2007,** *104* (36), 14215-14220.

7. Saavedra, J.; Doan, H. A.; Pursell, C. J.; Grabow, L. C.; Chandler, B. D., The critical role of water at the gold-titania interface in catalytic CO oxidation. *Science* **2014,** *345* (6204), 1599-1602.

8. Liu, Z.-P.; Hu, P.; Alavi, A., Catalytic Role of Gold in Gold-Based Catalysts: A Density Functional Theory Study on the CO Oxidation on Gold. *J. Am. Chem. Soc.* **2002,** *124* (49), 14770-14779.

9. Remediakis, I. N.; Lopez, N.; Norskov, J. K., CO oxidation on rutile-supported Au nanoparticles. *Angew. Chem., Int. Ed.* **2005,** *44* (12), 1824-1826.

10. Janssens, T. V. W.; Clausen, B. S.; Hvolbaek, B.; Falsig, H.; Christensen, C. H.; Bligaard, T.; Norskov, J. K., Insights into the reactivity of supported Au nanoparticles: combining theory and experiments. *Topics in Catalysis* **2007,** *44*, 15-26.

11. Molina, L. M.; Rasmussen, M. D.; Hammer, B., Adsorption of O2 and oxidation of CO at Au nanoparticles supported by TiO2(110). *J. Chem. Phys.* **2004,** *120* (16), 7673-7680.

12. Kim, H. Y.; Lee, H. M.; Henkelman, G., CO Oxidation Mechanism on CeO2-Supported Au Nanoparticles. *J. Am. Chem. Soc.* **2012,** *134* (3), 1560-1570.

13. Wang, Y.-G.; Yoon, Y.; Glezakou, V.-A.; Li, J.; Rousseau, R., The Role of Reducible Oxide-Metal Cluster Charge Transfer in Catalytic Processes: New Insights on the Catalytic Mechanism of CO Oxidation on Au/TiO2 from ab Initio Molecular Dynamics. *J. Am. Chem. Soc.* **2013,** *135* (29), 10673-10683.